

# CMOS Transistor Scaling Past 32nm and Implications on Variation

Kelin J. Kuhn

Intel Corporation, Portland Technology Development

RA3-353, 2501 NW 229<sup>th</sup> Ave., Hillsboro, OR 97124 (kelin.ptd.kuhn@intel.com)

**Abstract -** This paper explores CMOS transistor scaling past the 32nm generation and its implications on variation. Front-end variation sources are reviewed, with detailed discussion on lithography and polish variation sources past 32nm. New transistor architectures are discussed, with emphasis on benefits and challenges relative to variation. Detailed variation measurement techniques are reviewed, with supporting multi-generational trend results, including data from the 32nm node.

## I. INTRODUCTION

For the past 40 years, relentless focus on Moore's Law transistor scaling has delivered ever-increasing transistor density. For much of that time, Moore's Law transistor scaling meant "classic" Dennard scaling [1] where oxide thickness ( $T_{ox}$ ), transistor length ( $L_g$ ) and transistor width ( $W$ ) were scaled by a constant factor ( $1/k$ ) in order to provide a delay improvement of  $1/k$  at constant power density. In recent years, Dennard scaling has become less influential, and performance enhancers have been added to continue the density scaling roadmap (e-SiGe and strained SiN for strain in the 90nm and 65nm nodes [2,3], and high-k metal-gate (HiK-MG) in the 45nm and 32nm nodes [4,5]). As a consequence of continued density scaling, features are moving ever closer to fundamental dimensions (such as atomic dimensions and light wavelengths) meaning that management of variation will play a major role in future technology scaling [6].

## II. VARIATION SOURCES

Variation sources in the CMOS front-end [7, and references therein] can be categorized into two groups. The first group consists of historical variation sources which will continue to offer challenges moving forward. This group includes patterning proximity effects (both classical, and optical proximity correction (OPC) [8]), line-edge and line-width roughness (LER and LWR, respectively [9]), polish variations (shallow trench isolation (STI) [10] and gate [11]), and variations in the gate dielectric (oxide thickness variations [12], fixed charge [13], and defects and traps [14]). The second group includes variation sources which were historically of minor impact, but have emerged as significant challenges in recent years. This group includes random dopant fluctuation (RDF) [15-17], variation associated with implants and anneals (tool-based [18], pocket implants [19], rapid-thermal anneal (RTA) [20]), variation associated with strain (wafer-level biaxial [21], high-stress capping layers [22], and embedded silicon-germanium (SiGe) [23]) and variation associated with granularity in the gate material (for poly gates, [24], for metal gates, [25]).

## A. Patterning past 32nm

The last four technology generations have used 193nm optical lithography, with OPC, aperture improvement, advanced lens designs, and immersion lithography bridging the resolution gap (see Fig. 1).

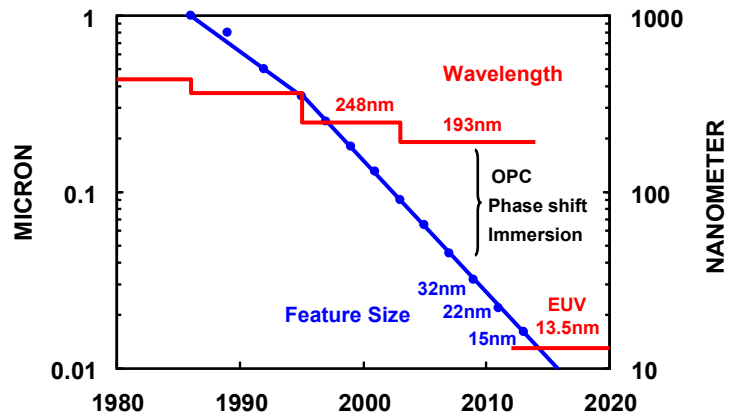


Fig. 1. Recent technology generations have used 193nm optical lithography, with OPC, aperture improvement, advanced lens designs, and immersion lithography bridging the resolution gap.

The effectiveness of these advanced lithography techniques can be seen in the steady improvement in gate critical dimension (CD) variation (see Fig. 2) as well as the steady reduction in SRAM cell area (see Fig. 3).

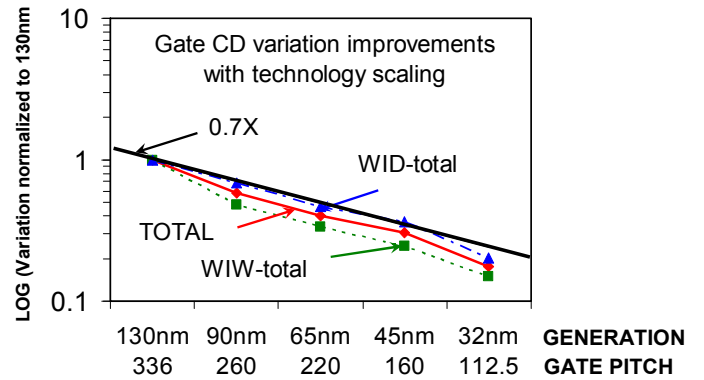


Fig. 2. Critical to management of variation is the ability to deliver a 0.7X gate CD variation improvement in each generation enabled by continuous process technology improvements [26].

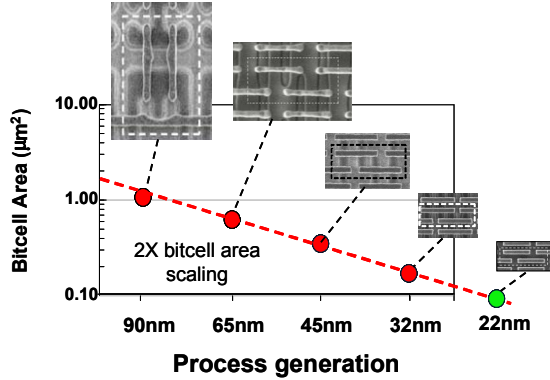


Fig. 3. Consistent 2X bitcell area scaling for the last five generations [27].

While there is certainly much discussion and anticipation on the generational intercept point for EUV lithography, perhaps of more interest to the variation community are the non-EUV pitch-reduction technologies. These technologies (such as double-patterning, or spacer-patterning) are likely to alter historical variation trends (and will undoubtedly be paired with EUV in advanced technology nodes.)

Double patterning technologies decrease the pitch by patterning twice, either through a resist freeze technique, or a double pattern transfer. These techniques allow for pitch-doubling without EUV technology. However, double patterning techniques still require resolution of a very small space (with associated LER and LWR issues), are very sensitive to misalignment between the two exposures (see Fig. 4-left), and eliminate the close correlation between adjacent transistor pairs (with significant implications for memory cells and other circuits that rely on CD matching between adjacent devices, see Fig. 4-right).

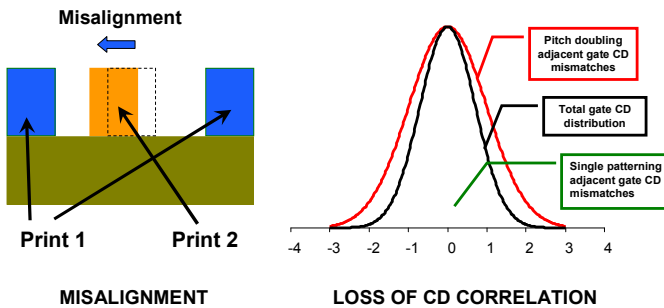


Fig. 4. Challenges of double patterning [26].

Spacer patterning technologies decrease the pitch by patterning a dummy structure at 2X the desired pitch, depositing spacers on the dummy structure, and then removing the dummy to leave the spacers at the desired pitch. Spacer patterning allows for significant pitch reduction without EUV technology, and does not suffer from misalignment or correlation issues. However, spacer patterning poses significant integration challenges and likely requires a “trim” mask (Fig. 5).

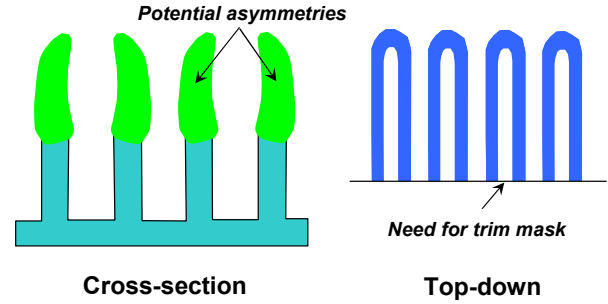


Fig. 5. Spacer patterning will have variation and integration challenges.

#### B. Polish past 32nm

Of particular interest are historical variation sources whose impact has been altered by advanced processing. An excellent example is the polish operations associated with the replacement gate high-k metal gate process.

Recall that there are two primary competing architectures for high-k metal gate (Fig. 6). These are gate first (where the metal is laid down before gate definition) and replacement gate (where a sacrificial gate is fabricated and later replaced by the metal gate material) [4, 28-29].

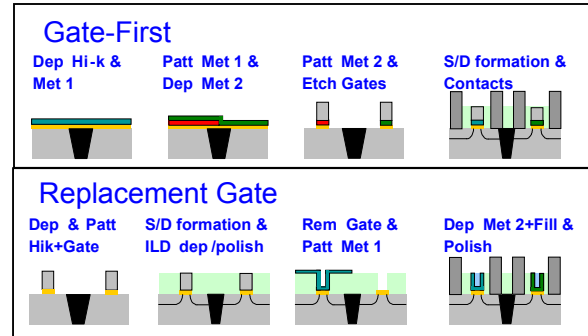


Fig. 6. HiK-MG flows, gate first vs. replacement gate [28]

The replacement gate process has several benefits over the gate-first process. One benefit is that replacement gate permits higher temperature anneals prior to the metal deposition (for better activation of implants). Another benefit is that the replacement gate flow enables an elegant PMOS strain enhancement mechanism (Fig. 7) through first straining the PMOS with e-SiGe and then removing the gate [28,30].

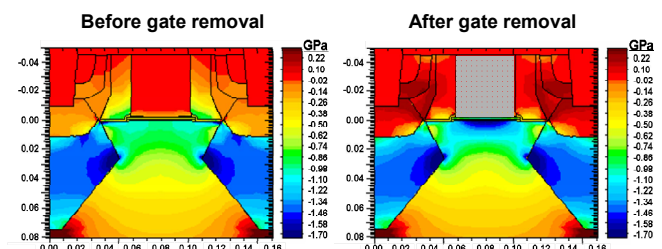


Fig. 7. Removal of poly gate increases channel stress by 50% [28].

However, the replacement gate process also poses challenges, as it requires two new polishing steps and interacts with STI polish (see Fig. 8).

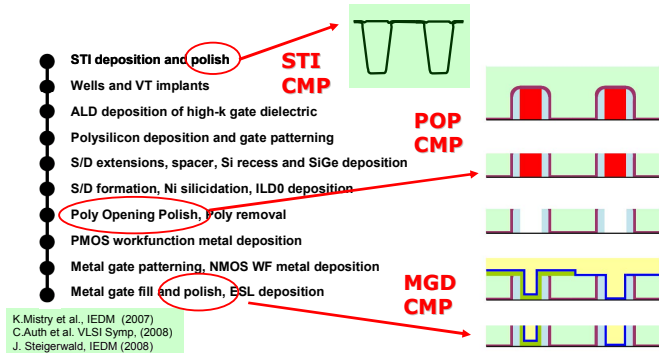


Fig. 8. Replacement metal gate: three critical CMP operations [11].

Gate height control is essential in a replacement gate process (see Fig. 9). If the gate is over-polished, the raised source-drain is exposed to the polish, resulting in  $R_{ext}$  and mobility variation. If the gate is under-polished, the contact taper causes  $R_{ext}$  variation (the extreme case resulting in an open-contact yield issue).

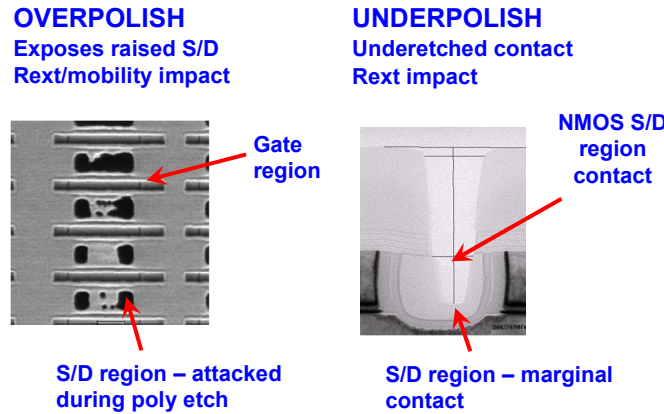


Fig. 9. Criticality of gate-height control in a replacement gate process [11].

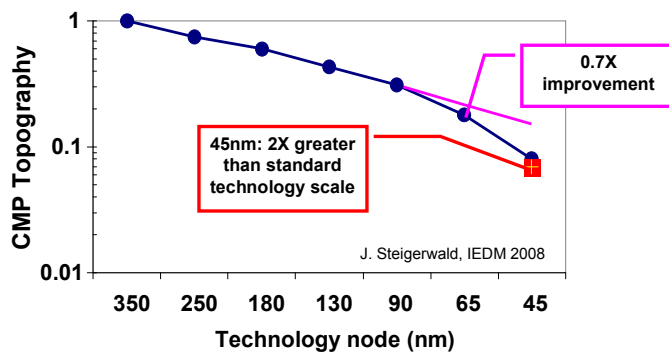


Fig. 10. 2X improvement in the topography roadmap associated with the introduction of the replacement gate process [11].

To avoid an increase in variation, the developmental roadmap for gate polish improvement needs to exceed 0.7X technology scaling in the generation where the replacement gate process is introduced. This is illustrated in Fig. 10, where the 45nm generation (the first introduction of replacement metal gate in manufacturing) shows almost a 2X improvement over the standard 0.7X generational scaling.

### III. FUTURE TRANSISTOR ARCHITECTURES

A variety of device architectures are being investigated for advanced technology nodes. These architectures can be broadly categorized by the method of electrostatic confinement. There are architectures which provide additional electrostatic confinement with a planar architecture (ultra-thin body (UTB), fully-depleted SOI (FDSOI), etc.), those which use 1'D electrostatic confinement (double gate, FinFET, etc.), those with more than 1'D, but less than 2'D (Trigate, Omega-FET, etc.) and those with full 2'D confinement (gate-all-around (GAA), nanowire etc.) [31].

#### A. Additional electrostatic confinement in planar

The potential value of fully-depleted UTB SOI for planar electrostatic confinement (as well as the requirements for extremely Si thin layers to achieve well-designed fully-depleted devices) has been recognized since the mid-1980s [32-33]. There has been a steady reduction in the minimum demonstrated body thicknesses ( $T_{si}$ ) moving from ~100nm in the 1980s and early 90s [34-35], down to the 15-20nm range in early 2000 [36-38], and more recently to values significantly below 10nm [39-41].

UTB SOI devices benefit from using similar manufacturing to planar SOI technology, but with improved SCE, potential for improved RDF (due to lower channel doping) and the possibility for body bias (with thin BOX).

Challenges of UTB SOI include thin  $T_{si}$  effects (external resistance,  $R_{ext}$ , scattering, and quantum confinement changes in  $V_T$ ), difficulties in inducing strain and variation manufacturing challenges with the thin  $T_{si}$ .

#### B. 1'D and 1'D+ confinement

There is a tradeoff between the electrostatic improvement of a GAA device and the fabrication complexity of making gates on all sides of a channel. A number of intermediate architectures (sometimes called multiple gate FET devices or MuGFETs) have been developed in an attempt to get the best SCE with the minimum process complexity [42-59].

Double-gate devices first appeared in the literature in the mid-1980s [42], and a variety of different geometries were explored in the next two decades [43-58]. Categories (see Fig. 11) include:

FinFET: Combines double-gate and vertical device concepts for a more manufacturable version of a double gate device [44-55].

**Trigate:** Differs from FinFETs in the absence of a gate-blocking layer on the top of the gate. Trigate devices have gates around three sides of the device, providing improved SCE with reduced vertical topography requirements [56-57].

**Pi-gates:** Differs from Trigates in having the gate extend below the channel. This creates a virtual back gate which shields the back of the channel from electric field lines from the drain, providing improved SCE [58].

**Omega-FETs:** Differ from Trigates in that the gate not only wraps around three sides, but underlaps part of the fourth. This has an effect similar to Pi-gate in shielding the back of the channel from field lines, resulting in improved SCE [59].

All of these multiple-gate devices have similar RDF and SCE advantages over planar as UTB SOI. In addition, the increased confinement in comparison with UTB devices relaxes the manufacturing constraints ( $W_{si} \sim 2T_{si}$ ). Furthermore, tying the gates together provides nearly ideal sub-threshold slope. Note also that independent gate operation is possible in some of these architectures.

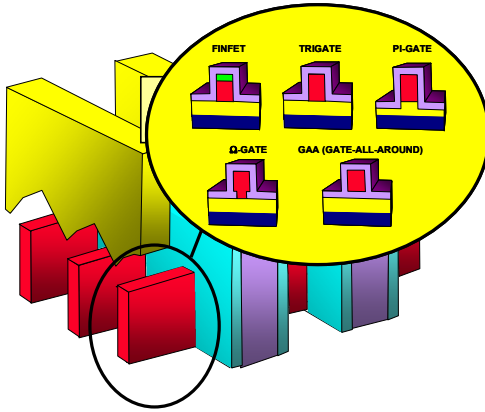


Fig. 11. Type of multiple gate architectures.

MuGFETs share the strain and  $R_{ext}$  challenges of UTB devices. In addition, these devices face significant variation challenges posed by the vertical topography, tight diffusion pitches and complex gate patterning.

### C. 2'D confinement

GAA devices were first reported in the late 1990s [60-61]. GAA devices differ from Omega-FETs in that the gate wraps entirely around the device. Note that both lateral [60,62,64], and vertical [61,63], devices are possible with this architecture. Both types provide full two dimensional confinement with the associated RDF and SCE benefits.

GAA devices offer the best potential solution to electrostatic confinement challenges of future devices, as well as offering the possibility for significant RDF reduction. However, these devices face significant challenges. Not only do they have the strain,  $R_{ext}$ , vertical topography, tight pitch, and complex gate patterning challenges of the MuGFET devices, they also face new challenges with gate conformality and excess parasitic capacitance.

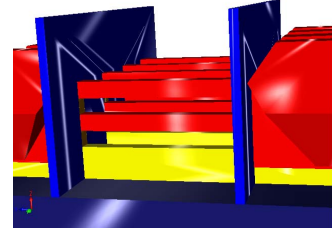


Fig. 12. Nanowires are an extreme case of GAA devices.

Nanowires are an extreme case of GAA devices, having height and width dimensions roughly the same (or even cylindrical) and small (<10nm) dimensions [Fig. 12, 65-69]. Nanowires add the challenges of phonon scattering [70], (along with possible benefits due to reduction in interface scattering [71-72]).

### III. VARIATION DEFINITIONS AND MEASUREMENT STRATEGIES

Unfortunately, the terms “random variation” and “systematic variation” do not have a unified definition in the semiconductor variation community. Experimentally, random variation can be defined as the variation measured between a pair of two closely-spaced objects. Systematic variation can be defined as the variation measured from a number of widely separated objects, after the random variation has been removed by a root-mean-square (RMS) analysis (eq. 1).

$$\sigma X_{\text{systematic}} = \sqrt{(\sigma X_{\text{pop}})^2 - (\sigma X_{\text{random}})^2} \quad (1)$$

Using  $V_T$  as an example, the most common way to measure random variation ( $\sigma V_T$ ) is to measure the difference in  $V_T$  ( $DV_T$ ) between paired closely spaced devices, obtain the standard deviation of  $DV_T$  ( $\sigma DV_T$ ) over a large population of pairs (for example, all the pairs on a wafer), divide  $\sigma DV_T$  by  $\sqrt{2}$  to obtain the random  $\sigma V_T$  for the individual device as,

$$\sigma V_{T_{\text{one-device(random)}}} = \frac{\sigma(VT_A - VT_B)}{\sqrt{2}} = \frac{\sigma(DVT)}{\sqrt{2}} \quad (2)$$

then, compute the systematic  $\sigma V_T$  from the RMS as,

$$\sigma V_{T_{\text{systematic}}} = \sqrt{(\sigma V_{T_{\text{pop}}})^2 - \left(\frac{\sigma(DVT)}{\sqrt{2}}\right)^2}. \quad (3)$$

One significant difficulty with the paired-device method is that there may be systematic variation of the random variation. (As one common example, the random variation measured from matched pairs may be systematically higher at the edge of the wafer than in the center) Unfortunately, the obvious mitigation (filtering the data) carries the associated risk of

dropping the sample size below good statistical sampling criteria as defined by the central limit theorem (CLT). (As a common example of this problem, if statistical data is evaluated on a per-wafer basis, under-sampling can result in the measured  $\sigma$  varying from wafer to wafer solely due to the under-sampling – not the underlying process.)

One way to address under-sampling issues with paired devices is to use measurement arrays (see Fig. 13 and 14). A measurement array consists of a large number of devices, each individually addressable, so all parametric measurements ( $V_T$ ,  $I_D$ ,  $SS$ ,  $DIBL$ , etc.) can be done on a large set of closely-spaced devices. The size of the array is chosen so as to be large enough to avoid CLT sampling issues, but smaller than all known systematic effects (typically  $100 < \text{array size} < 1000$ ). The clear value of these arrays is they provide  $\sigma X$  values for a single physical test structure (essentially a single physical location on the wafer). The disadvantage is that arrays have systematic layout debiasing (see Fig. 13) and significant testing analysis and effort is required to accurately measure arrays.

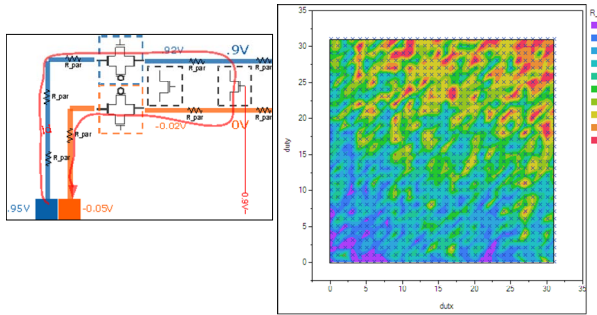


Fig. 13. Systematic parasitic resistance variation across an array structure

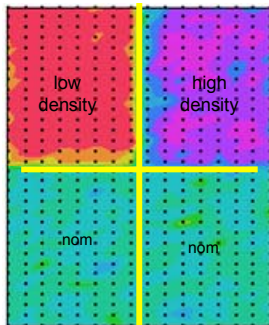


Fig. 14. Use of a bias-compensated array to measure variation in precision resistors as a function of pattern density.

Another approach for variation measurement is to use ring oscillators (see Fig. 15). By analogy with individual devices (eq. 1), closely spaced ring oscillators (or ring oscillators with interlaced transistors) are used to obtain random variation data, and large populations of oscillators (with random variation removed via RMS) are used to obtain systematic variation data.

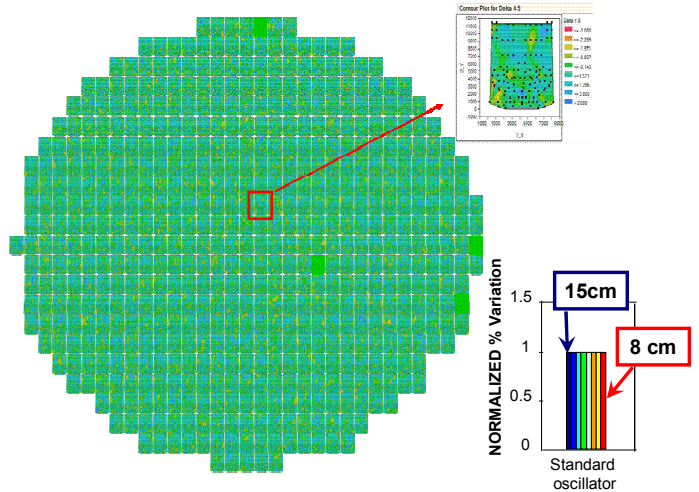


Fig. 15. Use of a ring-oscillators to measure random variation across a 45nm product wafer [7]

The positive features of ring oscillators are that they can be implemented on product die rather than test chip die (frequency data can be easily multiplexed out with other end-of-line tests on product material). The value of product implementation is a dramatic increase in the sample size.

The major negative feature of ring oscillators is the difficulty in correlating the measured frequency variation back to simple parametric terms (such as  $V_T$ ,  $I_D$ ,  $SS$ ,  $DIBL$ , etc.), or individual process mechanisms (such as  $L_e$ , mobility,  $R_{sd}$  etc.). In spite of these difficulties, product ring oscillators remain an excellent way to benchmark overall product variation between technologies, as they represent a simple circuit design than can be implemented generation after generation (see Fig. 16)

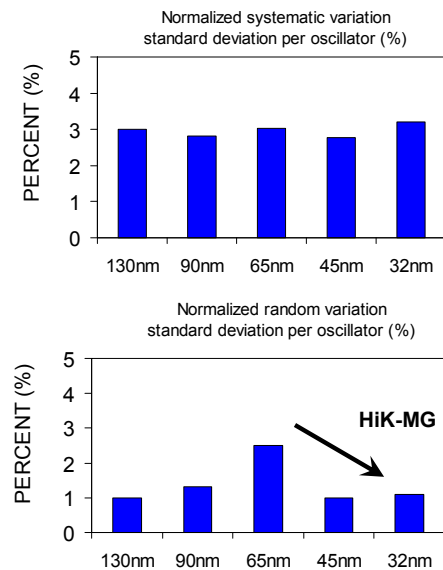


Fig. 16. Systematic variation (top) and random variation (bottom). Technology trends for the last five generations [7].

#### IV. CONCLUSION

While significant variation challenges exist for technologies past 32nm, numerous solutions are being explored to drive Moore's Law forward. Process variation is not an insurmountable barrier to Moore's law, but is simply another challenge to be overcome.

#### REFERENCES

- [1] Dennard, R. et al., "Design of ion-implanted MOSFET's with very small physical dimensions," IEEE Journal of Solid-State Circuits, Vol. 9, No. 5, pp. 256-268, Oct 1974.
- [2] Thompson, S. et al., "A 90 nm logic technology featuring 50 nm strained silicon channel transistors, 7 layers of Cu interconnects, low k ILD, and 1  $\mu\text{m}^2$  SRAM cell," IEDM Tech. Dig., pp. 61-64, Dec. 2002.
- [3] Bai, P. et al., "A 65nm logic technology featuring 35nm gate lengths, enhanced channel strain, 8 Cu interconnect layers, low-k ILD and 0.57  $\mu\text{m}^2$  SRAM cell," IEDM Tech. Dig., pp. 657-660, Dec. 2004.
- [4] Mistry, K. et al., "A 45nm Logic Technology with High-k+Metal Gate Transistors, Strained Silicon, 9 Cu Interconnect Layers, 193nm Dry Patterning, and 100% Pb-free Packaging," IEDM Tech. Dig., pp. 247-250, Dec. 2007.
- [5] Natarajan, S. et al., "A 32nm logic technology featuring 2nd-generation high-k + metal-gate transistors, enhanced channel strain and 0.171 $\mu\text{m}^2$  SRAM cell size in a 291Mb array," IEDM Tech. Dig., pp. 941-943, Dec. 2008.
- [6] Kuhn, Klein J., "Reducing Variation in Advanced Logic Technologies: Approaches to Process and Design for Manufacturability of Nanoscale CMOS," IEEE International Electron Devices Meeting, IEDM Technical Digest, December 2007, pp. 471-474.
- [7] Kuhn, K., et al., "Managing Process Variation in Intel's 45nm CMOS Technology", Intel Technical Journal, Vol. 12, No. 2, June 17, 2008.
- [8] L. Capodieci, "From optical proximity correction to lithography-driven physical design (1996-2006): 10 years of resolution enhancement technology and the roadmap enablers for the next decade." In Proceedings SPIE Volume. 6154, 615401.
- [9] Asenov, A., Brown, A.R., Davies, J.H., Kaya, S., & Slavcheva, G., "Intrinsic parameter fluctuations in decanometer MOSFETs introduced by gate line edge roughness," IEEE Transactions on Electron Devices, Volume 50, Issue 5, May 2003, pp. 1254-1260.
- [10] Nag, S., Chatterjee, A., Taylor, K., Ali, I., O'Brien, S., Aur, S., Luttmmer, J.D., & Chen, I.C., "Comparative evaluation of gap-fil dielectrics in shallow trench isolation for sub-0.25  $\mu\text{m}$  technologies," IEEE International Electron Devices Meeting, IEDM Technical Digest, December 1996, pp. 841-845.
- [11] Steigerwald, J., "Chemical mechanical polish: The enabling technology," IEEE International Electron Devices Meeting, IEDM Technical Digest, December 2008, 37-40.
- [12] M. Koh et al., "Limit of gate oxide thickness scaling in MOSFETs due to apparent threshold voltage fluctuation introduced by tunnelling leakage current," IEEE Transactions on Electron Devices, Volume 48, Issue 1, January 2001, pp. 259-264.
- [13] Kaushik, V.S. et al., "Estimation of fixed charge densities in hafnium-silicate gate dielectrics," IEEE Transactions on Electron Devices, Volume 53, Issue 10, October 2006, pp. 2627-2633.
- [14] Wen, H. C. et al., "On Oxygen Deficiency and Fast Transient Charge-Trapping Effects in High-k Dielectrics," IEEE Electron Device Letters, Volume 27, Issue 12, December 2006, pp. 984-987.
- [15] P. Stolk, F. Widdershoven and D. Klaassen, "Modeling statistical dopant fluctuations in MOS transistors," IEEE Transactions on Electron Devices, Volume 45, Issue 9, September 1998, pp. 1960-1971.
- [16] Takeuchi, K. et al., "Understanding Random Threshold Voltage Fluctuation by Comparing Multiple Fabs and Technologies," IEEE International Electron Devices Meeting, IEDM Technical Digest, December 2007, pp. 467-470.
- [17] A. Asenov, "Random dopant induced threshold voltage lowering and fluctuations in sub-0.1  $\mu\text{m}$  MOSFETs: A 3-D "atomatic simulation study," IEEE Transactions on Electron Devices, Volume 45, Issue 12, December 1998, pp. 2505-2513.
- [18] Al-Bayati et al., "Advanced CMOS device sensitivity to USJ processes and the required accuracy of doping and activation." In Proceedings of the 14th International Conference on Ion Implantation Technology, September 22-27, 2002, pp. 185-188.
- [19] Tanaka, T. et al., "Vth fluctuation induced by statistical variation of pocket dopant profile," IEEE International Electron Devices Meeting, IEDM Technical Digest, December 2000, pp. 271-274.
- [20] Ahsan, I. et al., "RTA-Driven Intra-Die Variations in Stage Delay, and Parametric Sensitivities for 65nm Technology," 2006 Symposium on VLSI Technology, Digest of Technical Papers, June 2006, pp. 170-171.
- [21] Tsang, Y.L. et al., "Modeling of the Threshold Voltage in Strained Si/Si<sub>1-x</sub>GexSi<sub>1-y</sub>Gex CMOS Architectures," IEEE Transactions on Electron Devices, Volume 54, Issue 11, November 2007, pp. 3040-3048.
- [22] Weber, O. et al., "High immunity to threshold voltage variability in undoped ultra-thin FDSOI MOSFETs and its physical understanding," IEEE International Electron Devices Meeting, IEDM Technical Digest, December 2008, pp. 245-248.
- [23] Pang, L-T., et al., "Measurement and Analysis of Variability in 45 nm Strained-Si CMOS Technology," IEEE J. of Solid State Circuits, Vol. 44, No. 8, 2009, pp. 2233-2243.
- [24] Brown, A.R., Roy, G., & Asenov, A., "Poly-Si-Gate-Related Variability in Decanometer MOSFETs with conventional architecture, IEEE Transactions on Electron Devices, Volume 54, Issue 11, November 2007, pp. 3056-3063.
- [25] Zhang, Y. et al. "Physical model of the impact of metal grain work function variability on emerging dual metal gate MOSFETs and its implication for SRAM reliability," IEEE International Electron Devices Meeting, IEDM Technical Digest, December 2009, pp. 57-60.
- [26] Kuhn, K., "Variation in 45nm and Implications for 32nm and Beyond," 2009 2nd International CMOS Variability Conference, May 2009.
- [27] Kuhn, K., "Technology Options for 22nm and Beyond," 2010 International Workshop on Junction Technology (IWJT ), May 2010.
- [28] Auth, C. et al., "45nm High-k + metal gate strain-enhanced transistors," 2008 Symp. on VLSI Tech, pp.128-129, June 2008
- [29] Khare, Mukesh, "High-K/Metal Gate Technology: A New Horizon." IEEE Custom Integrated Circuits Conference, CICC '07, September 16-19, 2007 pp. 417-420.
- [30] Wang, J. et al. "Novel Channel-Stress Enhancement Technology with eSiGe S/D and Recessed Channel on Damascene Gate Process," 2007 IEEE Symposium on VLSI Technology, 12-14 June 2007 Page(s):46 - 47
- [31] Liu T.J.K., Chang, L., Into the Nano Era, Springer, Vol. 106, Chapter 8, 2009.
- [32] Lim, H.K., and Fossum, J.G., "Threshold voltage of thin-film Silicon-on-insulator (SOI) MOSFET's," IEEE Transactions on Electron Devices, Vol. 30, No. 10, pp. 1244-1251, 1983.
- [33] Colinge, J.P., "Transconductance of silicon-on-insulator MOSFETs", IEEE Electron Device Letters, vol. EDL-6, pp. 573-574, 1985
- [34] Colinge, J.P., "Subthreshold slope of thin-film SOI MOSFETs", IEEE Electron Device Letters, vol. EDL-7, pp. 244-246, 1986
- [35] Chan, M., et al, "Recess channel structure for reducing source/drain series resistance in ultra-thin SOI MOSFETs," IEEE International SOI Conference, pp. 172 – 173, 1993
- [36] Choi, Y.K., et al., "Ultrathin-body SOI MOSFET for deep-sub-tenth micron era", IEEE Electron Device Letters, Vol.: 21 , No. 5, pp. 254-255, 2000
- [37] Doris, B., et al, High performance FDSOI CMOS technology with metal gate and high-k," 2005 Symp. on VLSI Tech, pp.214-215, June 2005
- [38] Gallon, C., "Ultra-Thin Fully Depleted SOI Devices with Thin BOX, Ground Plane and Strained Liner Booster," IEEE International SOI Conference, pp. 17 – 18, 2006
- [39] Andrieu, F., et al., "25nm Short and Narrow Strained FDSOI with TiN/HfO<sub>2</sub> Gate Stack", 2006 Symp. on VLSI Tech, pp.134-135, June 2006
- [40] Barral, V., et al, Strained FDSOI CMOS technology scalability down to 2.5nm film thickness and 18nm gate length with a TiN/HfO<sub>2</sub> gate stack", IEDM Tech. Dig., pp. 61-64, Dec. 2007.
- [41] Cheng, K., Fully depleted extremely thin SOI technology fabricated by a novel integration scheme featuring implant-free, zero-silicon-loss, and faceted raised source/drain", 2009 Symp. on VLSI Tech, pp.212-213, June 2009
- [42] Balestra, F., et al., "Double-gate silicon-on-insulator transistor with volume inversion: A new device with greatly enhanced performance," IEEE Electron Device Letters, Vol. 8, No. 9 pp. 410-412, 1987.
- [43] Wong, H.-S.P., et al., "Self-aligned (top and bottom) double-gate MOSFET with a 25 nm thick silicon channel," IEDM Tech. Dig., pp. 427-430, Dec. 1997.
- [44] Hisamoto, D., et al., "A fully depleted lean-channel transistor (DELTA)-a novel vertical ultra thin SOI MOSFET," IEDM Tech. Dig., pp. 833-836, Dec. 1989.
- [45] Hisamoto, D., et al., "A fully depleted lean-channel transistor (DELTA)-a novel vertical ultrathin SOI MOSFET," IEEE Electron Device Letters, Vol. 11 , No. 1, pp. 36-38, 1990
- [46] Hisamoto, D., et al., "Impact of the vertical SOI 'DELTA' structure on planar device technology," IEEE Trans. on Electron Devices, Vol. 38 , No. 6, pp. 1419-1424, 1991.
- [47] Lee, J-H., et al., "Super self-aligned double-gate (SSDG) MOSFETs utilizing oxidation rate difference and selective epitaxy," IEDM Tech. Dig., pp. 71-41, Dec. 1999
- [48] Kedzierski, J., et al., "High-performance symmetric-gate and CMOS-compatible Vt asymmetric-gate FinFET devices," IEDM Tech. Dig., pp. 19.5.1-19.5.4, Dec. 2001
- [49] Guarini, K.W., et al., "Triple-self-aligned, planar double-gate MOSFETs: devices and circuits," IEDM Tech. Dig., pp. 19.2.1-19.1.4, Dec. 2001
- [50] Hisamoto, D., et al., "A folded-channel MOSFET for deep-sub-tenth micron era," IEDM Tech. Dig., pp. 1032 - 1034, Dec. 1998.
- [51] Verheyen, P., et al., "25% driveline current improvement for p-type multiple gate FET (MuGFET) devices by the introduction of recessed Si0.8Ge0.2 in the source and drain regions," 2005 Symp. on VLSI Tech, pp.194-195, June 2005
- [52] Collaert, et al., "Optimization of the MuGFET performance on Super Critical-Strained SOI (SC-SSOI) substrates featuring raised source/drain and dual CESL," VLSI-TSA 2007, pp. 1-2, 23-25 April 2007.
- [53] Vellianitis, G., et al., "Gatestacks for scalable high-performance FinFETs," 2007 Symp. on VLSI Tech, pp.681-684, June 2007.
- [54] Kang, Y.C., et al., "Effects of Film Stress Modulation Using TiN Metal Gate on Stress Engineering and Its Impact on Device Characteristics in Metal Gate/High-Dielectric SOI FinFETs," IEEE Electron Device Letters, vol. 29, no. 5, pp. 487-490, 2008.
- [55] Chang, Y-C., et al., "A 25-nm Gate-Length FinFET Transistor Module for 32nm Node", IEDM Tech. Dig., pp. 12.2.1-12.2.4, Dec. 2009 [83] Doyle, B., et al. "Tri-Gate fully-depleted CMOS transistors: fabrication, design and layout," 2003 Symp. on VLSI Tech, pp.133-134, June 2003
- [56] Doyle, B., et al. "High performance fully-depleted tri-gate CMOS transistors," IEEE Electron Device Letters, Vol. 24, No. 4, pp. 263-265, 2003.
- [57] Kavalieros, J., et al., "Tri-Gate Transistor Architecture with High-k Gate Dielectrics, Metal Gates and Strain Engineering," 2006 Symp. on VLSI Tech, pp.50-51, June 2006
- [58] Park, J-T., et al."Pi-Gate SOI MOSFET," IEEE Electron Device Letters, Vol. 22, No. 8, pp. 405-406, 2001.
- [59] Yang, F-L., "25 nm CMOS Omega FETs", IEDM Tech. Dig., pp. 255-258, Dec. 2002.
- [60] Colinge, J.P., et al., "Silicon-on-insulator 'gate-all-around device'", IEDM Tech. Dig., pp. 595-598, Dec. 1990.
- [61] Takato, H., et al., "Impact of surrounding gate transistor (SGT) for ultra-high-density LSIs," IEEE Transactions on Electron Devices, Vol. 38, No. 3, pp. 573-578, 1983.
- [62] Monfray, S., et al., "50 nm-Gate All Around (GAA)-Silicon On Nothing (SON)-devices: a simple way to co-integration of GAA transistors within bulk MOSFET process," 2002 Symp. on VLSI Tech, pp.108-109, June 2002
- [63] Hergenrother, J.M., "The Vertical Replacement-Gate (VRG) MOSFET: a 50-nm vertical MOSFET with lithography-independent gate length," IEDM Tech. Dig., pp. 75-78, Dec. 1999.
- [64] Oh, S-H., et al., "Analytic description of short-channel effects in fully-depleted double-gate and cylindrical, surrounding-gate MOSFETs," IEEE Electron Device Letters, Vol.: 21 , No. 9, pp. 445-447, 2000
- [65] Suk, S.D., et al., "High performance 5nm radius Twin Silicon Nanowire MOSFET (TSNWFET) : fabrication on bulk si wafer, characteristics, and reliability," IEDM Tech. Dig., pp. 717-720, Dec. 2005.
- [66] Yeo, K.H., et al., "Gate-All-Around (GAA) Twin Silicon Nanowire MOSFET (TSNWFET) with 15 nm Length Gate and 4 nm Radius Nanowires," IEDM Tech. Dig., pp. 539-542, Dec. 2006.
- [67] Dupre, C., et al., "15nm-diameter 3D stacked nanowires with independent gates operation: FFET," IEDM Tech. Dig., pp. 749-752, Dec. 2008.
- [68] Li, M., et al., "Sub-10 nm gate-all-around CMOS nanowire transistors on bulk Si substrate," 2009 Symp. on VLSI Tech, pp.94-95, June 2009.
- [69] Bangsaruntip, S., et al., "High Performance and Highly Uniform Gate-All-Around Silicon Nanowire MOSFETs with Wire Size Dependent Scaling," IEDM Tech. Dig., pp. 12.3-1-12.3-4, Dec. 2009.
- [70] Jin, S-H., et al., "Modeling of electron mobility in gated silicon nanowires at room temperature: Surface roughness scattering, dielectric screening, and band nonparabolicity," J. Appl. Phys. 102, 083715 (2007).
- [71] Kotlyar, R., et al., "Assessment of room-temperature phonon-limited mobility in gated silicon nanowires," App. Phys. Lett., Vol. 84, No. 25, pp. 5270-3, June 21, 2004.
- [72] Wang, J., et al, Theoretical investigation of surface roughness scattering in silicon nanowire transistors, App. Phys. Lett., Vol. 87, 043101 (2005)